

A Large-scale Interpretable Multi-modality Benchmark for Facial Image Forgery Localization

Jingchun Lian
Xi'an Jiaotong University
Xi'an, China

Yujiao Wu
CSIRO
Australia

Lingyu Liu
Xi'an Jiaotong University
Xi'an, China

Li Zhu
Xi'an Jiaotong University
Xi'an, China

Yaxiong Wang
Hefei University of Technology
Hefei, China

Zhedong Zheng
University of Macau
Macau, China

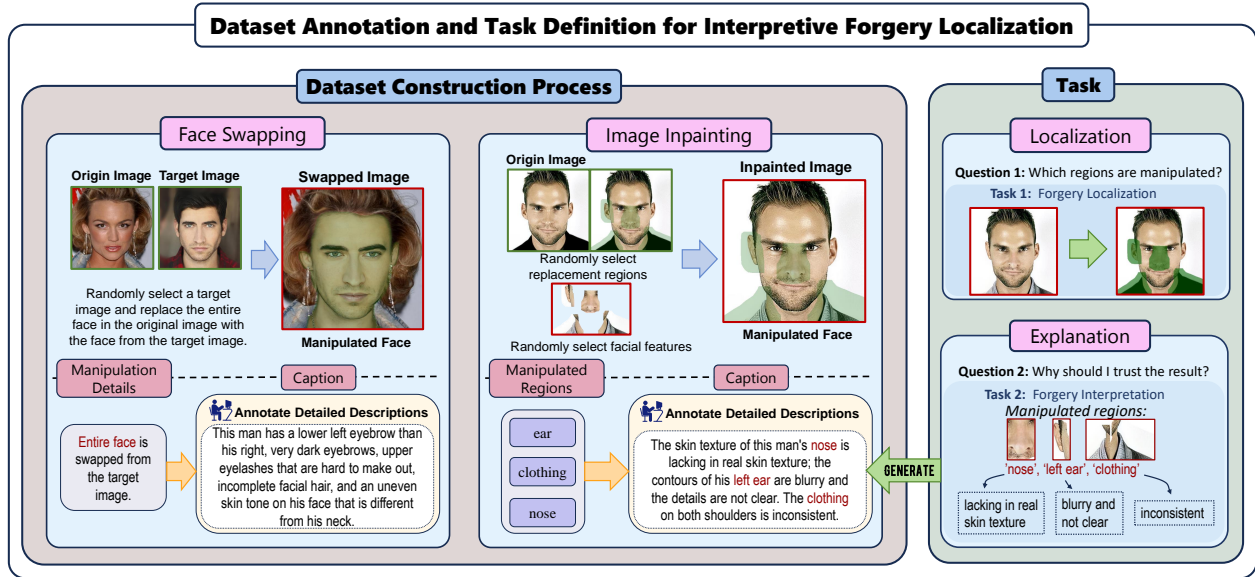


Figure 1. The proposed framework combines forgery localization and interpretive analysis. The left panel illustrates dataset construction with Face Swapping and Image Inpainting methods. The right panel defines tasks: forgery localization to identify manipulated regions and forgery interpretation to explain the manipulations, enhancing interpretability.

Abstract

Image forgery localization, which centers on identifying tampered pixels within an image, has seen significant advancements. Traditional approaches often model this challenge as a variant of image segmentation, treating the binary segmentation of forged areas as the end product. We argue that the basic binary forgery mask is inadequate for explaining model predictions. It doesn't clarify why the model pinpoints certain areas and treats all forged pixels the same, making it hard to spot the most fake-looking parts. In this study, we mitigate the aforementioned limitations by generating salient region-focused interpretation for the

forgery images. To support this, we craft a **Multi-Modal Trampler Tracing (MMTT)** dataset, comprising facial images manipulated using deepfake techniques and paired with manual, interpretable textual annotations. To harvest high-quality annotation, annotators are instructed to meticulously observe the manipulated images and articulate the typical characteristics of the forgery regions. Subsequently, we collect a dataset of 128,303 image-text pairs. Leveraging the MMTT dataset, we develop **ForgeryTalker**, an architecture designed for concurrent forgery localization and interpretation. **ForgeryTalker** first trains a forgery prompter network to identify the pivotal clues within the explanatory text. Subsequently, the region prompter is incorporated into

multimodal large language model for finetuning to achieve the dual goals of localization and interpretation. Extensive experiments conducted on the MMTT dataset verify the superior performance of our proposed model. The dataset, code as well as pretrained checkpoints will be made publicly available to facilitate further research and ensure the reproducibility of our results.

1. Introduction

The emergence of advanced generative models, particularly diffusion models [9, 34], has significantly enhanced the sophistication and realism of image generation techniques, making them increasingly difficult to detect. While these techniques have demonstrated immense potential in creative fields such as digital art and film production [5], they have also raised profound concerns about their misuse in malicious contexts, including misinformation campaigns and privacy violations [24, 29], especially the manipulation of facial images. Given these threats, DeepFake detection techniques have garnered significant attention and have rapidly evolved in recent years. Recent studies are shifting from simple real-fake detection to fine-grained forgery region localization to address the growing complexity of modern forgery techniques [32, 36, 37, 39].

Unlike binary classification methods, which merely determine whether an image is fake or real, forgery localization segments the exact areas that have been tampered with [36], aiming to explain the reason behind a forgery determination. Despite the recent significant strides in forgery localization, current methods still lack the ability to provide clear, interpretable justifications for their detections.

Binary masks, which merely highlight tampered pixels, provide limited insights into the rationale behind the model’s predictions [32]. Furthermore, these masks fail to differentiate between subtle and more significant alterations, treating all manipulated pixels equally, which often obscures the most critical areas that warrant closer scrutiny. Meanwhile, modern forgeries are often visually indistinguishable from real images. This makes it challenging for even human reviewers to identify tampered regions. For example, slight modifications in facial features, such as subtle distortions of the eyes or lips, are often overlooked in existing works, providing human observers with insufficient information to recognize the most anomalous regions. Given this, current models require additional outputs beyond binary masks to better reveal forged areas.

Based on the considerations outlined above, this work aims to develop an interpretable image forgery localization framework, including two abilities of segmenting the forgery pixels and generating interpretations for the tampered pixels. To enable the construction of such a framework, we first create a large-scale Multi-Modal Tampering

Tracing (MMTT) dataset, as shown in Figure 1, comprising image-text pairs of forgery images and the corresponding textual annotations. In specific, the MMTT dataset, focusing on face images and consisting of 128,303 forged facial samples, contains manipulated images that pose more threats to public information and privacy. Each image undergoes various manipulations, and the pixel-level forgery mask is automatically generated from the manipulation processes. To annotate the textual descriptions, we adopt a human-in-the-loop approach. Annotators first observe each forged image alongside its original version and are asked to pinpoint specific altered regions and describe the changes in detail. For each forged area, the type of manipulation (e.g., blurring, unnatural texture, or geometry distortion) is documented to ensure precise interpretability. The descriptions are iteratively refined through repeated inspection and feedback, ensuring that each annotation accurately captures even subtle alterations in the tampered regions, thereby enhancing the interpretability and quality of the dataset. This structured annotation procedure provides high-quality textual interpretations for the manipulations, offering a distinct advantage over existing datasets that typically lack such detailed contextual information.

With the MMTT dataset established, we design a framework, dubbed ForgeryTalker, to simultaneously perform forgery localization and generate interpretive reports for the manipulated regions. The overall architecture includes three primary components: the Forgery Prompter Network, a Mask Decoder, and a Multimodal Large Language Model (MLLM) as the backbone. The Forgery Prompter Network analyzes the manipulated features within the image and produces a concise yet informative prompt, capturing the core artificial characteristics of the forgeries. This prompt provides crucial priors for subsequent reasoning and makes the generation of a coherent explanation significantly easier. The Mask Decoder refines the pixel-level predictions, ensuring that only the most prominent manipulated regions are emphasized. Finally, the Language-based Explanation Module utilizes the generated prompt to articulate a coherent report that accurately captures the rationale behind the predicted forgery mask, addressing the inherent limitations of traditional binary segmentation approaches. Through the integration of these three components, our model not only achieves precise forgery localization but also provides contextually rich, human-understandable interpretation reports of the detected manipulations. Our contributions include:

- We make an early study for an unexplored problem, *i.e.*, interpretable forgery localization. A Multi-Modal Tampering Tracing (MMTT) dataset is collected to support the exploration of this problem, consisting of 128,303 forged facial image-text pairs. Each image is annotated with interpretable textual reasons, and paired with a corresponding forgery mask.

- This study establishes a baseline for addressing this new problem, named *ForgeryTalker*. *ForgeryTalker* first trains a forgery prompter to offer initial salient region clues and then fine-tune a multimodal large-language model to generate localization mask and interpretive report.

2. Related Work

2.1. Interpretation Annotation.

Facial Manipulation Localization. Detecting manipulated facial regions, especially deepfakes, has garnered attention. CNN-based methods [33] utilize temporal inconsistencies for videos, while GAN-based approaches, such as GAN-printR [26] and MaskGAN [23], address synthetic artifacts. Hybrid models like HCiT [12] combine CNNs and ViTs to enhance generalization, and multi-modal methods [14, 35] leverage spatial-temporal inconsistencies. However, these models lack interpretability and fine-grained mask generation, which our work addresses by providing both localization masks and textual explanations.

Multi-label Classification for Facial Localization. Multi-label classification captures independent alterations in facial regions but struggles with dependencies across features. CNNs [18] face limitations in fine-grained tasks, while hybrid models [12] improve detection by combining local and global features. Weighted loss functions [28] and parallel branches [30] address class imbalance and refine detection. Yet, few works integrate multi-label classification with localization. Our ViT-based classifier bridges this gap by capturing complex dependencies with parallel branches and weighted loss functions.

Segmentation Techniques. Segmentation is crucial for identifying localized manipulations. Models like U-Net and DeepLab [31] focus on spatial features, while Transformer models [2] capture global context. Recent methods like SAM [16] use a Two-Way Transformer for high-quality masks but lack manipulation-specific context. By integrating SAM with InstructBLIP, we create context-aware forgery masks, unifying segmentation and manipulation detection for enhanced localization.

3. Multi-Modal Trumper Tracing dataset

Although many existing datasets provide annotations for forgery localization, they lack detailed, descriptive explanations for the detected manipulations. To bridge this gap, we introduce the **Multi-Modal Trumper Tracing (MMTT)** dataset, which uniquely combines pixel-level forgery masks with comprehensive textual descriptions. Unlike conventional datasets that focus solely on binary classification [6, 22] or mask-based localization [11, 32], MMTT emphasizes interpretability by integrating annotations that explain how and why the manipulated regions appear forged. This

emphasis on human-generated interpretations allows for a richer understanding of the manipulations.

3.1. Source Image Collection

We develop our MMTT dataset based on the CelebAMask-HQ (CelebA-HQ) [42] and Flickr-Faces-HQ (FFHQ) [13] datasets. Both datasets offer high-quality, high-resolution facial images, CelebAMask-HQ containing 30,000 images and FFHQ providing 70,000 images, totaling 100,000 samples. All images are resized to 512×512 pixels for uniformity. The selected 100,000 images serve as the primary dataset for our subsequent forgery manipulations.

3.2. Forgery Generation

Generation and editing are two main threats for the face image protection. We incorporate both techniques for forgery image generation to construct a more challenging dataset. To keep pace with the latest techniques, we employ three manipulation methods: **face swapping** [1], along with **image inpainting** techniques, which include both **transformer-based** [21] and **diffusion-based methods** [27], to produce a comprehensive forgery dataset.

Face Swapping. For the face swapping task, we employ E4S [1], a GAN-based model designed specifically for high-quality face swapping. Given a target image I_t and a source image I_s , E4S generates a swapped face image I_f by replacing the entire face region in I_t with the facial features from I_s . For the CelebA-HQ dataset, target and source images are randomly paired from the entire dataset, while for FFHQ, the source image is chosen from a separate subfolder to maintain visual diversity.

During the swapping process, E4S automatically generates a binary mask M , which covers the entire face region of the target image I_t . This dynamically generated mask is used to blend facial features from I_s into I_t , ensuring the swapped image I_f only alters the facial region and preserves non-facial elements like hair and background from the target image.

The generated binary mask M is stored as the ground-truth annotation for the altered regions, representing the full face replacement for both CelebA-HQ and FFHQ datasets. As a result, the final outputs include both the forged images I_f and their corresponding binary masks M , providing a consistent representation of the modified regions for subsequent training and evaluation tasks.

Image Inpainting. For generating localized facial manipulations, we utilize MAT [21] (transformer-based) and SDXL [27] (diffusion-based).

For each image I , the process commences by defining a binary mask M that indicates the regions to be inpainted. Depending on the dataset, the process of mask generation varies. For the CelebAMask-HQ dataset, which contains predefined masks for 21 facial components (e.g., eyes, nose,

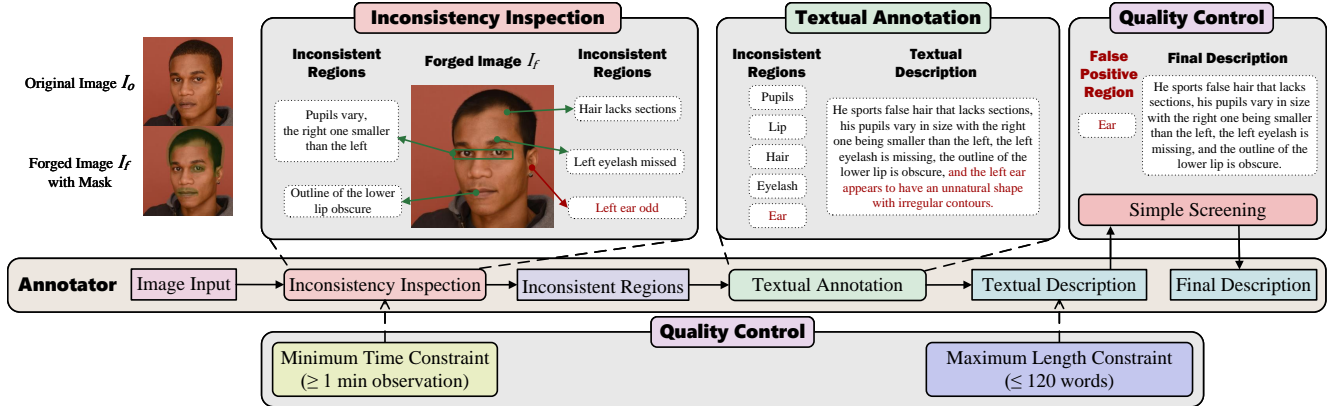


Figure 2. Annotation pipeline for forgery interpretation. Annotators review the original and forged images (I_o , I_f), conduct an Inconsistency Inspection with a Minimum Time Constraint (≥ 1 min), and identify Inconsistent Regions. These regions are used to produce Textual Descriptions within a Maximum Length Constraint (≤ 120 words). Quality Control then screens for false positives (e.g., Ear), ensuring only accurate descriptions are included in the Final Description.

Dataset	Reference	Task	Modality	Pristine Samp.	Uniq. Fake Samp.	Manipulation Types	GT Type	Text Anno.
Celeb-DF [22]	CVPR20	Cls.	Video	590	5,639	DeepFake	Image label	×
FaceForensics++ [32]	ICCV19	Seg. + Cls.	Video	1,000	4,000	Multi-Face Mods	Image label + Mask	×
DFDC [6]	arXiv20	Cls.	Video	23,654	104,500	DeepFake	Image label	×
DeeperForensics-1.0 [11]	CVPR20	Cls.	Video	50,000	10,000	GAN	Image label	×
DiffusionFace [3]	arXiv24	Gen.	Image	N/A	50,000	Diffusion	Image label	×
GenFace [41]	IEEE TIFS24	Gen.	Image	10,000	10,000	GAN, Inpainting	Mask	×
OpenForensics [19]	CVPR21	Det. + Seg.	Image + Video	45,473	70,325	GAN, Inpainting	BBox / Mask	×
ForgeryNet [8]	CVPR21	Cls. + Seg.	Video + Image	116,321	221,247	DeepFake, GAN	Image label + Mask	×
FaceShifter [20]	CVPR20	Cls.	Video	N/A	5,000	GAN	Image label	×
DF40 [38]	NeurIPS24	Cls. + Seg.	Image + Video	N/A	1,000,000+	Multi-Face Mods	Image label + Mask	×
MMTT (Ours)	-	Seg. + Cap.	Text + Image	100,000	128,303	GAN, Inpainting	Mask, Text	✓

Table 1. Comparison of face forgery datasets and attributes. ‘Cls.’, ‘Det.’, ‘Seg.’, ‘Cap.’, and ‘Gen.’ represent classification, detection, segmentation, captioning, and generation, respectively. Pristine samples are original images/videos used to generate forgeries, while unique fake samples count distinct fake instances. Text Annotation indicates whether detailed textual descriptions are included. The ‘Reference’ column specifies the publication venue and year. ‘Uniq.’, ‘Samp.’ and ‘Anno.’ mean ‘Unique’, ‘Sample’ and ‘Annotation’, respectively.

mouth, and eyebrows), we randomly select between 1 to 11 facial regions for modification. Specifically, we generate a random number k within this range, representing the number of facial parts to be altered. These regions are then randomly sampled and merged to create the final mask M . And for the Flickr-Faces-HQ dataset, which lacks predefined facial masks, we employ Dlib [15] to detect key facial landmarks. This allows us to segment the face into different regions such as eyebrows, eyes, nose, mouth, ears, and the entire face. For each image, we randomly determine if a full face mask is applied with a 20% chance. Otherwise, we pick k areas (with k ranging randomly from 1 to 11) to create the final mask M .

With the mask M determined, the image I is processed using the respective inpainting method. The masked image $I \cdot (1 - M)$ and its binary mask M are fed into the inpainting model, which predicts the missing pixels I_g^{model} for the masked regions, resulting in the inpainted image: $I_f = (1 - M) \cdot I + M \cdot I_g^{\text{model}}$, where $\text{model} = \{\text{MAT}, \text{SDXL}\}$.

Annotation Guidance. Figure 2 shows the pipeline of our

annotation process. To ensure the annotation quality, our expert team manually provides interpretations. The goal is to produce explanations that interpret the localization of forgeries and emphasize the most conspicuously artificial areas. As shown in Figure 2, annotators are presented with both the original and manipulated images, with the manipulated areas indicated by the groundtruth mask. They are instructed as follows:

- Carefully examine the pair of images and thoroughly describe any irregularities or artificial appearances found in the manipulated regions.
- Focus on accurately annotating only the unnatural or poorly integrated facial features, disregarding any areas that appear authentic.
- Avoid using language that requires reference to the original image, as this is not feasible in practical scenarios.
- Keep descriptions concise, limiting them to no more than 120 words.

Annotation Process. The annotation process involves 30 annotators. As shown in Figure 2, each annotator is pre-

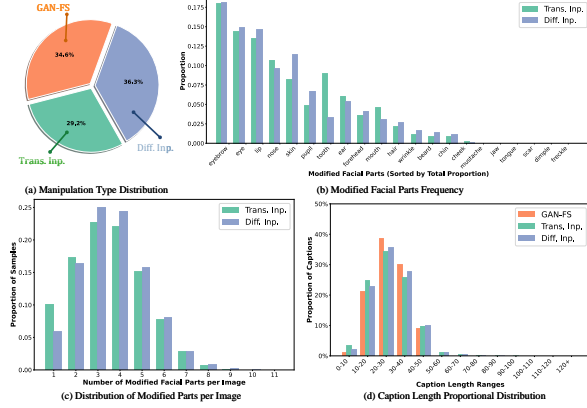


Figure 3. Overview of the MMTT dataset statistics. GAN-FS represents GAN-based Face Swapping, Trans. Inp. denotes Transformer-based Inpainting, and Diff. Inp. refers to Diffusion-based Inpainting. (a) shows the distribution of manipulation methods; (b) shows modified facial part frequency for each inpainting method (excluding GAN-FS, which involves full-face edits); (c) shows the distribution of modified parts per image for Transformer- and Diffusion-based inpainting (excluding GAN-FS due to no localized edits); (d) shows caption length distribution for all methods.

sented with the original image I_o and the forged image I_f , and asked to compare them. Based on the comparison and the annotation guidance, they identify and annotate the regions in I_f that exhibit unnatural or illogical alterations. The steps in the annotation process are as follows:

- **Step 1:** Annotators are given an original-forgery image pair (I_o, I_f) .
- **Step 2:** Annotators examine the images for inconsistencies in facial regions, such as unusual textures, asymmetry, or irregular shading.
- **Step 3:** Annotators provide a detailed textual description T , explaining the specific nature of the alteration (e.g., "The nose texture appears unnaturally smooth, lacking real skin details.").

Integrating all above annotated clues, each annotated sample in our MMTT dataset is finally formed as a triplet $p = (I_f, M, T)$.

To ensure dataset accuracy and consistency, the annotation process was conducted in two phases. From September 1 to November 3, 2023, annotators labeled around 20 images per hour, completing the primary dataset. A second phase from March 25 to July 26, 2024, reviewed and refined suboptimal annotations, resulting in high-quality, reliable labels for the MMTT dataset.

Annotation Quality Control. To ensure the quality of the annotations, strict quality control measures are applied:

- **Minimum Annotation Time.** Each annotator is required to spend at least one minute on each image, ensuring a thorough examination of the details in both I_o and I_f .

- **Simple Screening.** We conduct a basic screening of the annotations. If annotators label regions that were not manipulated, we remove those labels to ensure accuracy.

3.3. Dataset Statistics

The MMTT dataset D consists of **128,303** triplets, each represented by a forged face image, a binary mask, and a corresponding caption. The dataset is generated using three primary methods: GAN-based face swapping (44,343 samples), Transformer-based inpainting (37,440 samples), and Diffusion-based inpainting (46,520 samples).

Image Statistics: As shown in Figure 3, the most frequently manipulated regions in the entire dataset are the Eye (66,403), Eyebrow (83,594), and Lip (61,844). For example, in the transformer-based inpainting samples, the Eyebrow (22,993) and Eye (18,484) regions are particularly emphasized, accounting for 61.4% and 49.3% of the total images in this category, respectively. In contrast, diffusion-based methods, which are known for superior texture generation, target regions such as the Lip (24,483) and Eye (25,014), covering 52.6% and 53.8% of its samples.

Additionally, by combining both transformer-based and diffusion-based manipulation methods, the dataset reveals that: 21.7% of images have three modifications, 22.4% of samples contain four modified regions, and 17.4% of samples exhibit five regions altered simultaneously. This varied distribution increases the difficulty of forgery localization tasks, as models must effectively handle varying levels of complexity across different manipulation techniques.

Interpretation Statistics: In terms of textual annotations, the average caption length is 26.94 words, with the longest caption containing 123 words and the shortest having only 3 words. The total word count for all captions reaches 3,456,202, further underscoring the depth and comprehensiveness of the annotations.

Captions in the GAN-based category frequently mention regions such as Eye (38,399) and Eyebrow (30,454), reflecting their prominence in face-swapping operations. In transformer-based and diffusion-based methods, the Eye and Lip regions appear most often, with 30,487 and 24,516 mentions, respectively. Overall, the Eye (108,750) and Eyebrow (83,606) regions are the most frequently described, constituting over 84.6% of all textual references.

4. ForgeryTalker

4.1. Architecture

Our framework, ForgeryTalker, extends the InstructBlip [4] model by introducing a Forgery Prompter Network (FPN) and a Mask Decoder. The system accepts a tampered image I and encodes it into patch embeddings following Vision Transformer [7]. These embeddings are first processed by the Q-former, and the resulting features undergo cross at-

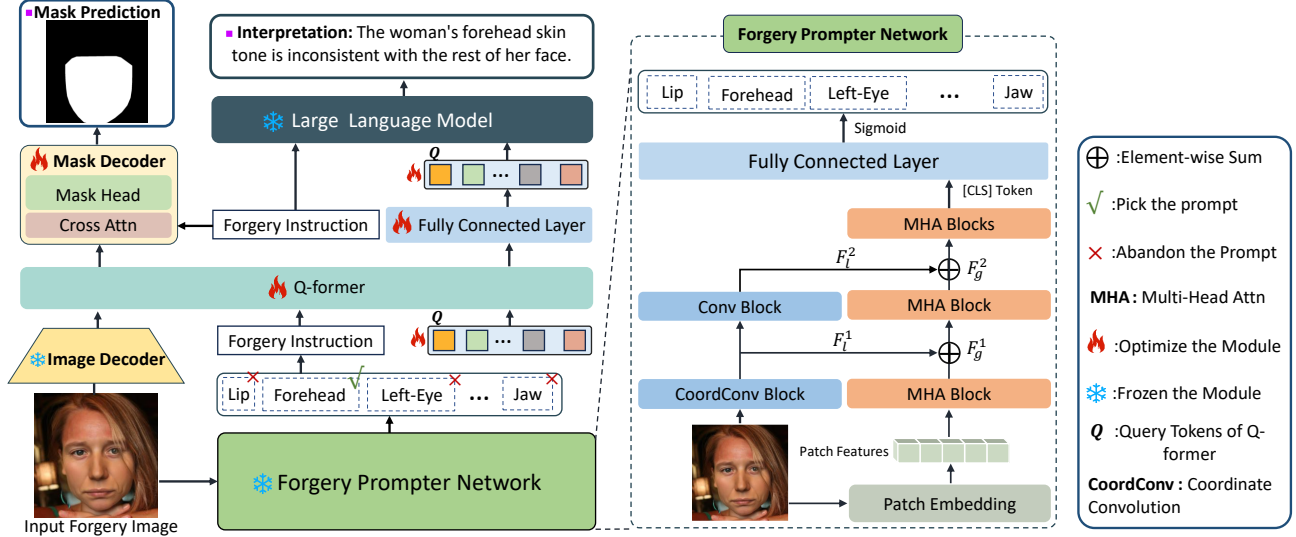


Figure 4. Illustration of our ForgeryTalker. ForgeryTalker extends the InstructBlip framework by incorporating a Forgery Prompter Network (FPN) and a Mask Decoder. The framework processes an image into patch embeddings via a Vision Transformer. These embeddings are refined by the Q-former, whose features then interact with FPN’s regional prompts through cross attention for forgery localization in the mask decoder. The FPN generates region prompts, merged with an instruction template and fed into the Q-former. In the second stage, the FPN is frozen, while the mask decoder and Q-former are jointly optimized for segmentation and language generation. The multimodal features are passed to a large language model to produce a descriptive explanation of the forgery.

tention with FPN’s region prompts before being fed to the mask decoder for localization. The FPN is initially trained to produce region prompts, which are then combined with an instruction template and fed into the Q-former of InstructBlip. The ensuing multimodal features are channeled through a large language model to produce an interpretive narrative of the forgery. The training is performed in a two-stage fashion: initially, the FPN is trained with a classification loss, followed by a second phase where the FPN is fixed while the mask decoder and Q-former are collectively optimized with segmentation and language generation losses.

4.2. Forgery Prompter Network

Motivation. Accurately identifying the most salient manipulated regions in forged images is difficult due to the high visual fidelity of modern manipulation techniques. Even human reviewers often need to inspect the image closely to spot inconsistencies. Thus, we propose the Forgery Prompter Network to provide an initial set of salient region keywords, guiding the downstream reasoning and facilitating the coherent generation of explanations.

GroundTruth Extraction. We extract region labels from our interpretation annotations. The label space consists of 21 face semantics, with each image’s label as a 21-dimensional vector Y , where the i -th position is 1 if the corresponding face part is in the interpretation, 0 otherwise. **FPN** takes the vision transformers as the main architecture. Considering the crucial role of fine-grained local context in

identifying subtle flaws, we introduce a convolution branch at the early m layers to complement the global contexts captured by the vision transformer. As shown in Figure 4, the forgery image I concurrently traverses self-attention blocks and convolution blocks in parallel, producing global-aware features $F_g = \{F_g^0, F_g^2, \dots, F_g^{m-1}\}$ and local-aware features $F_l = \{F_l^0, F_l^2, \dots, F_l^{m-1}\}$. At each encoding level, the corresponding features are element-wise summed and fed into next attention block:

$$F_g^i = \text{MHA}_{i-1}(F_g^{i-1}), F_l^i = \text{Conv}_{i-1}(F_l^{i-1}), \quad (1)$$

$$F_g^i = \text{MHA}_i(F_g^i + F_l^i), \quad i = 1, \dots, m \quad (2)$$

where “MHA” and “Conv” mean the multi-head attention and convolution, respectively. Furthermore, we note that the positioning of facial regions in a natural image follows a rigid and predictable structure, with the eyes typically positioned laterally relative to the nose and the eyebrows aligned above the eyes. Leveraging this regularity, we integrate coordinate convolution [25] in the initial convolutional layer to detect anomalies in the arrangement of facial features, *i.e.*, $\text{Conv}_0 = \text{CoorConv}$.

The resultant feature F_g^m contains both global and local contexts and is then fed into the subsequent multi-head attention blocks and a classification head to produce the probability \hat{Y} across regions, as well as being used in cross attention with Q-former features for enhanced forgery localization. Finally, the forgery prompter network is optimized by a combined loss, incorporating both Binary Cross-Entropy

(BCE) loss and Dice loss to effectively balance region classification and overlap precision:

$$\mathcal{L}_{BCE} = -\frac{1}{21} \sum_{i=1}^{21} Y_i \log \hat{Y}_i + \omega(1 - Y_i) \log(1 - \hat{Y}_i), \quad (3)$$

where ω is a discount factor set to $\omega < 1$ to address the imbalance due to the prevalence of unmodified regions.

The Dice loss is employed to measure the overlap between the predicted labels \hat{Y} and ground truth Y , ensuring that less frequent classes receive more attention:

$$\mathcal{L}_{Dice} = 1 - \frac{2 \sum_{i=1}^{21} Y_i \hat{Y}_i}{\sum_{i=1}^{21} Y_i + \sum_{i=1}^{21} \hat{Y}_i}. \quad (4)$$

The final loss function is defined as the average of the BCE and Dice losses:

$$\mathcal{L}_f = \frac{1}{2}(\mathcal{L}_{BCE} + \mathcal{L}_{Dice}). \quad (5)$$

4.3. Interpretation Generation

Subsequently, we fix the trained FPN network and take the region predictions from FPN as prior clues to aid both the interpretation generation and the cross attention process for improved forgery localization. Assume the set of regions from FPN is $R = \{r_1, r_2, \dots\}$, we next design a particular template to include R to form an interpretation-friendly instruction T :

These facial areas may be manipulated by AI: [R]. Please describe the specific issues in these areas.

The structured prompt serves as the guiding context for the language model, thereby ensuring that the final output accurately reflects the manipulations detected by the FPN. This integration enhances the interpretability and coherence of the generated explanations, offering a comprehensive understanding of the tampered regions. Subsequently, the instruction and the image embeddings into the Q-former and the resultant feature are fed into the large-language model to generate the interpretation text T , which is then supervised by language modeling loss:

$$\mathcal{L}_t = -\mathbb{E}_{(I,T) \sim \mathcal{D}} \left[\sum_{k=1}^K \log P(\hat{t}_k | (I, T), \hat{t}_0, \dots, \hat{t}_{k-1}) \right], \quad (6)$$

where \hat{t}_k is k -th predicted words, P is the word probability distribution from LLM.

4.4. Mask Decoder

We employ SAM’s Two-way Transformer [16] as the mask decoder. The image encoder of InstructBLIP encodes the forgery image. The resulting features from the Q-former are then enhanced through cross attention with

FPN’s regional prompts. These enriched features are subsequently fed into the Two-way Transformer to predict the forgery mask \hat{M} . The cross entropy loss is performed: $\mathcal{L}_m = -\frac{1}{HW} \log M_{ij} \log \hat{M}_{ij}$, where H, W is the height and width of image.

Overall, the full loss in the second stage for interpretation and forgery localization is formulated as:

$$\mathcal{L} = \mathcal{L}_t + \mathcal{L}_m. \quad (7)$$

5. Experiment

5.1. Experimental Setup

Implementation Details. We implement our ForgeryTalker framework using PyTorch and train it on four NVIDIA A100 GPUs. The Forgery Prompter Network is fine-tuned for 125,000 steps with a batch size of 16, an initial learning rate of $7.5e-3$, using a cosine decay strategy and warmup steps of 125. The convolution branch in FPN includes one 3×3 Coordinate Convolution (CoordConv) layer and one 5×5 Convolution layer. The discount factor in Eq. 3 is set as $\omega = 0.2$ to balance the unmodified regions. Next, we fix FPN and tune the Q-former and the mask decoder by 60 epochs, starting with a learning rate of $4e-6$. The training setup includes a batch size of 16 and a gradient accumulation strategy with an accumulation step of 1, with mixed-precision training (fp16) enabled for faster convergence and reduced memory usage. The Multi-Modal Tampering Tracing (MMTT) dataset is divided into training, validation, and test sets with a ratio of 8:1:1.

We use a range of captioning and segmentation metrics for performance evaluation, including CIDEr, BLEU, METEOR, and IoU. We use Positive Label Matching (PLM) to evaluate the effectiveness of FPN. PLM calculates the ratio of correctly predicted positive labels over the union of predicted and ground-truth positive labels:

$$PLM = \frac{|\text{Predicted Positive Labels} \cap \text{Ground Truth Positive Labels}|}{|\text{Predicted Positive Labels} \cup \text{Ground Truth Positive Labels}|}. \quad (8)$$

Unlike IoU, PLM focuses on detecting manipulated regions without being influenced by a large number of correctly predicted negative labels, making it ideal for tasks with sparse modifications.

5.2. Quantitative Results

As shown in Table 2, we compare our ForgeryTalker framework against several baseline models: SCA [10], LISA-7B [17], Osprey [40], and InstructBLIP [4].

In text generation, ForgeryTalker achieves the highest CIDEr score of 21.5, outperforming SCA’s 10.6, Osprey’s 9.2, and InstructBLIP’s 20.9. Additionally, ForgeryTalker surpasses InstructBLIP in BLEU-1 (31.1 vs. 30.6), BLEU-2 (16.9 vs. 16.8), and BLEU-4 (5.9 vs. 5.6), showcasing

Method	Reference	Interpretation Generation						Forgery Localization		
		CIDEr	BLEU-1	BLEU-2	BLEU-3	BLEU-4	ROUGE-L	IoU	Precision	Recall
SCA (GPT2-large) [10]	CVPR24	10.6	17.7	7.6	4.0	2.4	17.8	72.87	-	-
LISA-7B [17]	ICCV23	18.1	29.4	15.5	8.6	4.9	23.3	68.52	77.80	84.64
Osprey [40]	CVPR24	9.2	16.7	7.8	4.4	2.5	18.5	-	-	-
InstructBLIP [4]	NeurIPS23	20.9	30.6	16.8	9.8	5.6	24.8	67.38	85.47	80.25
ForgeryTalker	-	21.5	31.1	16.9	9.8	5.9	24.3	70.81	87.06	78.34

Table 2. Performance comparison of generated captions and forgery localization across models. "Interpretation Generation" metrics evaluate caption relevance and diversity, while "Forgery Localization" metrics assess accuracy in identifying tampered regions.

Method	Interpretation Generation						Forgery Localization		
	CIDEr	Bleu_1	Bleu_2	Bleu_3	Bleu_4	ROUGE_L	IoU	Precision	Recall
ForgeryTalker <i>w/</i> FPN-GT	48.1	38.0	22.4	14.4	9.5	32.3	70.26	88.83	77.93
ForgeryTalker <i>w/o</i> FPN	20.9	30.6	16.8	9.8	6.0	24.8	67.38	85.47	80.25
ForgeryTalker	21.5	31.1	16.9	9.8	5.9	24.3	70.81	87.06	78.34

Table 3. Ablation Study on the Impact of Different Variants. *w/* and *w/o* mean equipping or not equipping the following modules.

its ability to produce contextually rich and informative captions. LISA-7B performs competitively in most text metrics but trails slightly in CIDEr and BLEU-4, suggesting a limitation in generating highly detailed captions. In contrast, SCA and Osprey both yield significantly lower scores across text metrics due to generating overly simplistic and repetitive outputs, which fail to capture the nuanced contextual details needed for effective interpretation.

For forgery localization, ForgeryTalker achieves an IoU score of 70.81, which is comparable to SCA’s 72.87 and significantly higher than InstructBLIP’s 67.38. Although ForgeryTalker slightly underperforms SCA in IoU, this difference is largely attributed to SCA’s reliance on the Segment Anything Model (SAM), a framework specifically optimized for segmentation tasks that provides an edge in forgery localization. LISA-7B attains a high precision of 77.80 and recall of 84.64, but these scores remain below ForgeryTalker’s precision of 87.06, underscoring ForgeryTalker’s advantage in achieving precise localization. Since Osprey lacks the capability to output standalone forgery masks, its IoU and related localization metrics are not reported.

Overall, ForgeryTalker maintains a good balance between text generation and image segmentation tasks. Although some individual metrics favor other models, ForgeryTalker achieves better average performance across multiple evaluation criteria, demonstrating its robustness for detailed forgery analysis.

5.3. Ablation Study

We performed ablation experiments to analyze the effects of key components, focusing on text generation performance (CIDEr). As shown in Table 3, we study several variants:

w/ FPN-GT. Uses ground-truth labels instead of the predicted labels from the Forgery Prompter Network, achieving the best CIDEr score (48.1), indicating the value of precise label guidance.

w/o FPN. Removes Forgery Prompter Network, leading to a

Model	ω	Loss	PLM
ViT	1	BCE	34.23
ViT	0.2	BCE	38.92
FPN	0.2	BCE	39.16
FPN	0.2	BCE + Dice	41.05

Table 4. Ablation Study on the Impact of the FPN significant performance drop (CIDEr: 20.9), demonstrating the importance of our FPN.

The ground-truth (GT) labels show great potential to enhance the interpretation generation, achieving a CIDEr score of 48.1 (Table 3). This means that we can harvest high-quality interpretation if the region prompts are given accurately. FPN is motivated by this and targets to yield region prompts. The interpretation generation is hindered by FPN’s performance. As shown in Table 4, the PLM of FPN is only 41%, which has great potential to be improved and will be continually studied in our future work. Table 4 also discusses the discount hyperparameters factor ω (Eq. 3) and the loss configurations, the results reveals that the discounting the unmodified regions and equipping the BCE and Dice loss can both promote the accuracy of region prompts.

6. Conclusion

This paper addresses the limitations of traditional image forgery localization by developing an advanced framework that generates comprehensive interpretive reports for forged images. Existing binary forgery masks often lack the detail needed to convey model predictions and effectively highlight key forgery areas. To address this, we created the MMTT dataset with deepfake-manipulated images and corresponding textual annotations. Our proposed ForgeryTalker framework combines forgery localization with interpretive text generation to enhance both accuracy and transparency. Experiments on the MMTT dataset validate the model’s distinct advantages in forgery localization and interpretation.

References

- [1] Chafic Abou Akar, Rachele Abdel Massih, Anthony Yaghi, Joe Khalil, Marc Kamradt, and Abdallah Makhoul. Generative adversarial network applications in industry 4.0: A review. *International Journal of Computer Vision*, 132(6):2195–2254, 2024. 3
- [2] Dosovitskiy Alexey. An image is worth 16x16 words: Transformers for image recognition at scale. *arXiv preprint arXiv: 2010.11929*, 2020. 3
- [3] Zhongxi Chen, Ke Sun, Ziyin Zhou, Xianming Lin, Xiaoshuai Sun, Liujuan Cao, and Rongrong Ji. Diffusionface: Towards a comprehensive dataset for diffusion-based face forgery analysis. *arXiv preprint arXiv:2403.18471*, 2024. 4
- [4] Wenliang Dai, Junnan Li, Dongxu Li, Anthony Meng Huat Tiong, Junqi Zhao, Weisheng Wang, Boyang Li, Pascale Fung, and Steven Hoi. Instructblip: Towards general-purpose vision-language models with instruction tuning, 2023. 5, 7, 8
- [5] Prafulla Dhariwal and Alexander Nichol. Diffusion models beat gans on image synthesis. *Advances in neural information processing systems*, 34:8780–8794, 2021. 2
- [6] Brian Dolhansky, Joanna Bitton, Ben Pflaum, Jikuo Lu, Russ Howes, Menglin Wang, and Cristian Canton Ferrer. The deepfake detection challenge (dfdc) dataset. *arXiv preprint arXiv:2006.07397*, 2020. 3, 4
- [7] Alexey Dosovitskiy. An image is worth 16x16 words: Transformers for image recognition at scale. *arXiv preprint arXiv:2010.11929*, 2020. 5
- [8] Yinan He, Bei Gan, Siyu Chen, Yichun Zhou, Guojun Yin, Luchuan Song, Lu Sheng, Jing Shao, and Ziwei Liu. Forgerynet: A versatile benchmark for comprehensive forgery analysis. In *Proceedings of the IEEE/CVF conference on computer vision and pattern recognition*, pages 4360–4369, 2021. 4
- [9] Jonathan Ho, Ajay Jain, and Pieter Abbeel. Denoising diffusion probabilistic models. *Advances in neural information processing systems*, 33:6840–6851, 2020. 2
- [10] Xiaoke Huang, Jianfeng Wang, Yansong Tang, Zheng Zhang, Han Hu, Jiwen Lu, Lijuan Wang, and Zicheng Liu. Segment and caption anything. In *Proceedings of the IEEE/CVF Conference on Computer Vision and Pattern Recognition*, pages 13405–13417, 2024. 7, 8
- [11] Liming Jiang, Ren Li, Wayne Wu, Chen Qian, and Chen Change Loy. Deepforensics-1.0: A large-scale dataset for real-world face forgery detection. In *Proceedings of the IEEE/CVF conference on computer vision and pattern recognition*, pages 2889–2898, 2020. 3, 4
- [12] Bachir Kaddar, Sid Ahmed Fezza, Wassim Hamidouche, Zahid Akhtar, and Abdenour Hadid. Hcitr: Deepfake video detection using a hybrid model of cnn features and vision transformer. In *2021 International Conference on Visual Communications and Image Processing (VCIP)*, pages 1–5. IEEE, 2021. 3
- [13] Tero Karras, Samuli Laine, and Timo Aila. A style-based generator architecture for generative adversarial networks. In *Proceedings of the IEEE/CVF conference on computer vision and pattern recognition*, pages 4401–4410, 2019. 3
- [14] Atharva Khedkar, Atharva Peshkar, Ashlesha Nagdive, Mahendra Gaikwad, and Sudeep Baudha. Exploiting spatiotemporal inconsistencies to detect deepfake videos in the wild. In *2022 10th International Conference on Emerging Trends in Engineering and Technology-Signal and Information Processing (ICETET-SIP-22)*, pages 1–6. IEEE, 2022. 3
- [15] Davis E King. Dlib-ml: A machine learning toolkit. *The Journal of Machine Learning Research*, 10:1755–1758, 2009. 4
- [16] Alexander Kirillov, Eric Mintun, Nikhila Ravi, Hanzi Mao, Chloe Rolland, Laura Gustafson, Tete Xiao, Spencer Whitehead, Alexander C Berg, Wan-Yen Lo, et al. Segment anything. In *Proceedings of the IEEE/CVF International Conference on Computer Vision*, pages 4015–4026, 2023. 3, 7
- [17] Xin Lai, Zhuotao Tian, Yukang Chen, Yanwei Li, Yuhui Yuan, Shu Liu, and Jiaya Jia. Lisa: Reasoning segmentation via large language model. In *Proceedings of the IEEE/CVF Conference on Computer Vision and Pattern Recognition*, pages 9579–9589, 2024. 7, 8
- [18] S Lalitha and Kavitha Sooda. Deepfake detection through key video frame extraction using gan. In *2022 International Conference on Automation, Computing and Renewable Systems (ICACRS)*, pages 859–863. IEEE, 2022. 3
- [19] Trung-Nghia Le, Huy H Nguyen, Junichi Yamagishi, and Isao Echizen. Openforensics: Large-scale challenging dataset for multi-face forgery detection and segmentation in-the-wild. In *Proceedings of the IEEE/CVF international conference on computer vision*, pages 10117–10127, 2021. 4
- [20] Lingzhi Li, Jianmin Bao, Hao Yang, Dong Chen, and Fang Wen. Faceshifter: Towards high fidelity and occlusion aware face swapping. *arXiv preprint arXiv:1912.13457*, 2019. 4
- [21] Wenbo Li, Zhe Lin, Kun Zhou, Lu Qi, Yi Wang, and Jiaya Jia. Mat: Mask-aware transformer for large hole image inpainting. In *Proceedings of the IEEE/CVF conference on computer vision and pattern recognition*, pages 10758–10768, 2022. 3
- [22] Yuezun Li, Xin Yang, Pu Sun, Honggang Qi, and Siwei Lyu. Celeb-df: A large-scale challenging

- dataset for deepfake forensics. In *Proceedings of the IEEE/CVF conference on computer vision and pattern recognition*, pages 3207–3216, 2020. 3, 4
- [23] Dazhuang Liu, Zhen Yang, Ru Zhang, and Jianyi Liu. Maskgan: A facial fusion algorithm for deepfake image detection. In *2022 International Conference on Computers and Artificial Intelligence Technologies (CAIT)*, pages 71–78. IEEE, 2022. 3
- [24] Kunlin Liu, Ivan Perov, Daiheng Gao, Nikolay Chervoniy, Wenbo Zhou, and Weiming Zhang. Deepface-lab: Integrated, flexible and extensible face-swapping framework. *Pattern Recognition*, 141:109628, 2023. 2
- [25] Rosanne Liu, Joel Lehman, Piero Molino, Felipe Petroski Such, Eric Frank, Alex Sergeev, and Jason Yosinski. An intriguing failing of convolutional neural networks and the coordconv solution. *Advances in neural information processing systems*, 31, 2018. 6
- [26] Joao C Neves, Ruben Tolosana, Ruben Vera-Rodriguez, Vasco Lopes, Hugo Proença, and Julian Fierrez. Ganprint: Improved fakes and evaluation of the state of the art in face manipulation detection. *IEEE Journal of Selected Topics in Signal Processing*, 14(5):1038–1048, 2020. 3
- [27] Dustin Podell, Zion English, Kyle Lacey, Andreas Blattmann, Tim Dockhorn, Jonas Müller, Joe Penna, and Robin Rombach. Sdxl: Improving latent diffusion models for high-resolution image synthesis. *arXiv preprint arXiv:2307.01952*, 2023. 3
- [28] Sreeraj Ramachandran, Aakash Varma Nadimpalli, and Ajita Rattani. An experimental evaluation on deepfake detection using deep face recognition. In *2021 International Carnahan Conference on Security Technology (ICCST)*, pages 1–6. IEEE, 2021. 3
- [29] Md Shohel Rana, Mohammad Nur Nobil, Beddhu Murali, and Andrew H Sung. Deepfake detection: A systematic literature review. *IEEE access*, 10:25494–25513, 2022. 2
- [30] Mj Alben Richards, E Kaaviya Varshini, N Diviya, P Prakash, P Kasthuri, and A Sasithradevi. Deep fake face detection using convolutional neural networks. In *2023 12th International Conference on Advanced Computing (ICoAC)*, pages 1–5. IEEE, 2023. 3
- [31] T-YLPG Ross and GKHP Dollár. Focal loss for dense object detection. In *proceedings of the IEEE conference on computer vision and pattern recognition*, pages 2980–2988, 2017. 3
- [32] Andreas Rossler, Davide Cozzolino, Luisa Verdoliva, Christian Riess, Justus Thies, and Matthias Nießner. Faceforensics++: Learning to detect manipulated facial images. In *Proceedings of the IEEE/CVF international conference on computer vision*, pages 1–11, 2019. 2, 3, 4
- [33] Ekraam Sabir, Jiaxin Cheng, Ayush Jaiswal, Wael AbdAlmageed, Iacopo Masi, and Prem Natarajan. Recurrent convolutional strategies for face manipulation detection in videos. *Interfaces (GUI)*, 3(1):80–87, 2019. 3
- [34] Jiaming Song, Chenlin Meng, and Stefano Ermon. Denoising diffusion implicit models. *arXiv preprint arXiv:2010.02502*, 2020. 2
- [35] YuYang Sun, ZhiYong Zhang, Isao Echizen, Huy H Nguyen, ChangZhen Qiu, and Lu Sun. Face forgery detection based on facial region displacement trajectory series. In *Proceedings of the IEEE/CVF Winter Conference on Applications of Computer Vision*, pages 633–642, 2023. 3
- [36] Luisa Verdoliva. Media forensics and deepfakes: an overview. *IEEE journal of selected topics in signal processing*, 14(5):910–932, 2020. 2
- [37] Yuanlu Wu, Yan Wo, Caiyu Li, and Guoqiang Han. Learning domain-invariant representation for generalizing face forgery detection. *Computers & Security*, 130:103280, 2023. 2
- [38] Zhiyuan Yan, Taiping Yao, Shen Chen, Yandan Zhao, Xinghe Fu, Junwei Zhu, Donghao Luo, Chengjie Wang, Shouhong Ding, Yunsheng Wu, and Li Yuan. Df40: Toward next-generation deepfake detection, 2024. 4
- [39] Peipeng Yu, Zhihua Xia, Jianwei Fei, and Yujiang Lu. A survey on deepfake video detection. *Iet Biometrics*, 10(6):607–624, 2021. 2
- [40] Yuqian Yuan, Wentong Li, Jian Liu, Dongqi Tang, Xinjie Luo, Chi Qin, Lei Zhang, and Jianke Zhu. Osprey: Pixel understanding with visual instruction tuning. In *Proceedings of the IEEE/CVF Conference on Computer Vision and Pattern Recognition*, pages 28202–28211, 2024. 7, 8
- [41] Yaning Zhang, Zitong Yu, Tianyi Wang, Xiaobin Huang, Linlin Shen, Zan Gao, and Jianfeng Ren. Genface: A large-scale fine-grained face forgery benchmark and cross appearance-edge learning. *IEEE Transactions on Information Forensics and Security*, 2024. 4
- [42] Hao Zhu, Wayne Wu, Wentao Zhu, Liming Jiang, Siwei Tang, Li Zhang, Ziwei Liu, and Chen Change Loy. Celebv-hq: A large-scale video facial attributes dataset. In *European conference on computer vision*, pages 650–667. Springer, 2022. 3